

## Performance Evaluation of Advanced Wave Energy Converters in the Nearshore Areas of the North Indian Ocean

WAN Yong<sup>a,\*</sup>, ZHANG Wen<sup>a</sup>, FAN Chen-qing<sup>b</sup>, LI Li-gang<sup>a</sup>, DAI Yong-shou<sup>a</sup>

<sup>a</sup> The College of Oceanography and Space Informatics, China University of Petroleum, Qingdao 266580, China

<sup>b</sup> The Laboratory of Physical Oceanography and Remote Sensing, The First Institute of Oceanography, SOA, Qingdao 266061, China

Received March 7, 2022; revised August 8, 2022; accepted September 14, 2022

©2022 Chinese Ocean Engineering Society and Springer-Verlag GmbH Germany, part of Springer Nature

### Abstract

The 21st Century Maritime Silk Road is a profound measure for mankind, whilst its development is severely restricted by the energy shortage of surrounding countries. As the core construction area of Maritime Silk Road, the North Indian Ocean is rich in wave energy. The development and utilization of wave energy not only can overcome energy shortage, but also promote communication between peripheral countries. However, previous researchers often focused on wave energy itself, without combining devices to analyze wave energy resources. Therefore, we conducted an overall assessment of wave energy resources using 20-year ERA5 data and determined the sites considered as superior for the construction of Wave Energy Farm (WEF) in the coastal areas. In order to point out which type of Wave Energy Converter (WEC) is best suited for the sites, we carried out the performance evaluation of eight advanced WECs using three parameters: the mean power output, the capacity factor and the capture width ratio. The results show that the performance of Wave Star is superior to other devices, which is supposed to be the primary consideration of the Wave Energy Farms (WEFs) in the future.

**Key words:** ocean energy, wave energy characteristics, site selection, wave energy converter, performance evaluation

**Citation:** Wan, Y., Zhang, W., Fan, C. Q., Li, L. G., Dai, Y. S., 2022. Performance evaluation of advanced wave energy converters in the nearshore areas of the North Indian Ocean. *China Ocean Eng.*, 36(6): 980–993, doi: <https://doi.org/10.1007/s13344-022-0086-8>

### 1 Introduction

Nowadays, the excessive use of traditional fossil energy has led to the aggravation of global environmental pollution. In addition, the reserves of fossil energy are limited, and many countries have frictions due to the competition for fossil energy. Experts are eager to find a new way to solve this dilemma. The development of renewable sources of energy has become essential to mitigate the human influence on climate change (Ribeiro et al., 2021). As the top priority of the Belt and Road Initiative, the 21st Century Maritime Silk Road (Maritime Silk Road) plays a vital role in promoting equal communication, mutual cooperation and common prosperity among countries. The North Indian Ocean is regarded as the core construction area of the Maritime Silk Road, whose geographical location is important with irreplaceable economic and military strategic significance. However, the efficient development and in-depth promotion of the Maritime Silk Road exchanges have been seriously held back by the energy shortage and technological back-

wardness of the surrounding countries. In order to ensure a stable and sustainable energy supply, researchers have turned their attention to marine energy. The development and utilization of marine energy can not only overcome the energy shortage, but also promote communication between peripheral countries. Marine energy is renewable and non-polluting which is comprised of ocean thermal energy conversion, salinity gradients, current energy, tidal energy, and wave energy. Among them, wave energy has attracted much attention due to its cleanliness, large reserves and no pollution (Zheng and Li, 2017). There is no doubt that wave energy will be a hot spot for energy research in the world. At this time, the North Indian Ocean is rich in wave energy resources. The development of wave energy in the North Indian Ocean can not only alleviate the pressure of traditional fossil shortage, but also protect the ecological environment and promote sustainable development, which has far-reaching influence.

It is necessary to carry out wave energy assessments

Foundation item: The work was financially supported by the National Key R&D Program of China (Grant No. 2017YFC1405600), the National Natural Science Foundation of China (Grant No. 61931025) and Shandong Institute of Chinese Engineering S&T Strategy for Development (Grant No. 2022-DFZD-36).

\*Corresponding author. E-mail: [wanyong@upc.edu.cn](mailto:wanyong@upc.edu.cn)

before the development of wave energy resources. The assessments can not only estimate the reserves of wave energy, but also determine the advantageous development areas, providing clear guidance for the site selection of Wave Energy Farms (WEFs). In this way, we can exploit wave energy more efficiently. Mørk et al. (2010) evaluated the wave energy resources at a global scale. In addition, Reguero et al. (2015) used the mean wave power as the parameter to quantify the global wave energy and analyzed its stability. Iglesias et al. (2009) assessed the wave energy in Galicia to obtain the optimal energy production. Zheng et al. (2013) evaluated the wave energy of the China Sea based on the richness and stability. Zheng et al. (2019) developed a projection system for wave energy resources and assessed the wave energy in the South China Sea and the East China Sea. Akpınar and İhsan Kömürçü (2013) analyzed the wave energy resources of the Black Sea from the perspective of variability and determined that the southwest area of the Black Sea was most suitable for the development of wave energy. In addition, Rusu (2019) evaluated the near future wave energy resources of the Black Sea under different climates from 2021 to 2050. Liberti et al. (2013) evaluated the wave energy in the Mediterranean based on 10-year simulated data from wave model. Besio et al. (2016) also investigated the wave energy in the Mediterranean Sea from the perspective of variability based on 35-year wave hindcast data. Langodan et al. (2016) assessed wave energy of the Red Sea for development based on 18-year simulated data from the Advanced Weather Research Forecasting model. Zheng (2021) created the first global oceanic wave energy resource dataset for the first time, which filled the gap in this research area.

In addition, wave energy varies greatly with the distance from the shore. Therefore, it is necessary to analyze the wave energy resources in offshore and nearshore areas and determine the areas with the highest development potential. Accordingly, Iglesias et al. (2010) analyzed the wave energy in the coastal areas and offshore areas in Asturias. Langodan et al. (2016) assessed the wave energy from offshore sea areas to nearshore shallow areas for the Australian southeast shelf and determined the areas that were regarded the most promising for the development of wave energy. Lisboa et al. (2017) simulated the wave propagation process from offshore sea areas to nearshore shallow areas and analyzed the available wave energy resources in the nearshore and offshore areas of southern Brazil accordingly. Ahn et al. (2020) evaluated the wave energy in the nearshore areas of the US based on 30-year data from wave model. Amarouche et al. (2020) assessed the wave energy in the coastal waters of the Algerian basin using 39-year wave data. Ayob et al. (2017) estimated the wave energy potential in coastal waters of the Nordic countries. Saket and Etemad-Shahidi (2012) investigated the wave energy potential in the northern coastal waters of the Gulf of Oman and determined the areas where

the development potential was the highest. Patel et al. (2020) investigated the wave energy in the nearshore sea areas of Indian based on 19-year wave data and analyzed wave power resource at nine hotspot locations.

For the development of WEFs, it is far from enough to only assess the reserves and distribution of wave energy resources. The main device for collecting and converting wave energy is the wave energy converter (WEC). Therefore, wave energy assessments must be oriented to the actual wave energy converters (WECs) and the performance of different WECs should be compared. Researchers have carried out wave energy assessments combined with WECs. Koca et al. (2013) summarized the characteristics of several common WECs worldwide and introduced the most promising devices to date. Silva et al. (2013) assessed the wave energy in the coastal waters of Portugal and compared the performance of five WECs under the sea states of Portugal. Rusu (2014) assessed the wave power resources in three different types of coastal environment and compared the conversion efficiency of WECs at the key sites for the development of WEFs. Dalton et al. (2010) analyzed the Pelamis WEC at four different locations in terms of performance and economic feasibility. Andres et al. (2015) analyzed the applicability to climate conditions, productivity efficiency and economic performance of a generic WEC. Vannucchi and Cappietti (2016) estimated the wave energy resources in the offshore areas of the Mediterranean Sea combined with six various WECs and analyzed their applicability to the Italian sea areas. Bertram et al. (2020) developed a method for locating WEFs consisting of three main stages and selected the devices which matched the sites best. Wahyudie et al. (2020) assessed the wave energy resources in the south coast of the middle part of Java Island and selected the ideal sites for the placement of WECs. García-Medina et al. (2014) analyzed the variability of wave energy over the continental shelf in Oregon and southwest Washington, combining the feasibility of installation of WECs.

This paper presents a study assessing the wave energy potential from the prospective of richness and stability in the North Indian Ocean based on ERA5 wave data from 1999 to 2018 and investigating the performance of eight WECs at the sites which were considered as the ideal locations for WEFs in the nearshore areas of the North Indian Ocean. The results can be used as the basis for identifying the sites of WEFs in the inshore North Indian Ocean in the future.

## 2 Study area and dataset

### 2.1 Study area

As depicted in Fig. 1, the study area is the North Indian Ocean with a spatial range of 30°E–105°E and 15°S–30°N. The region is not only a vital part of the Pacific-Atlantic route, but also occupies a core position in the Maritime Silk Road. In addition, the North Indian Ocean is located in the

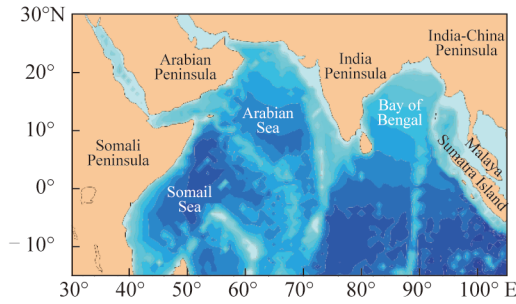


Fig. 1. Map of the study area.

low latitudes of subtropical zone, tropical zone and equator, adjacent to the African continent in the West, close to the Asian continent in the North and East, with three sides of the geographical situation surrounded by the continent. The temperature differs considerably from the vast continent to the adjacent ocean, consequently, the climate of the North Indian Ocean region is seriously affected by the interaction between sea and land, forming a significant monsoon climate. Chiu et al. (2013) have found that the northeast wind prevails in winter and the southwest wind blows in summer. Furthermore, the force and direction of the monsoon are very stable, but the southwest wind is wider and stronger than the northeast wind.

## 2.2 ERA5 data

The wave data are the ERA5 data provided by European Center for Medium-Range Weather Forecasts (ECMWF), with high spatio-temporal resolution and precise accuracy. The time range of this data employed in this study is from 1999 to 2018, and the spatial range is  $15^{\circ}\text{S}$ – $30^{\circ}\text{N}$  and  $30^{\circ}\text{E}$ – $105^{\circ}\text{E}$ . Furthermore, the temporal resolution is 6 h, and the spatial resolution is  $0.125^{\circ}\times 0.125^{\circ}$ . The ERA5 database, the fifth generation ECMWF re-analysis for the global climate and weather, is the product meets resolution and accuracy requirements. Wan et al. (2020) have compared the ERA-Interim data with buoy data, and they found that the ERA-Interim data had enough accuracy to be used as the base data for follow-up research. Hersbach et al. (2020) compared ERA5 data with ERA-Interim data using buoy observations and found that the ERA5 data was of better quality and more suitable for subsequent studies. To make assessments

more credible, we also compared the ERA5 data with some buoy data selected from the east-west coast of the United States. Specifically, we selected the significant wave height  $H_s$  and energy period  $T_e$  as the two parameters to carry out the accuracy evaluation.

As can be seen from Fig. 2, there is a good agreement between ERA5 data and buoy data. Furthermore, the root-mean-square-errors (RMSE) corresponding to significant wave height and energy period are 0.45 and 0.94. The scatter indexes (SI) are 0.25 m and 0.17, respectively. It can be seen that the ERA5 data have the precision high enough to be suitable for follow-up studies.

## 3 Methodology

We employed a systematic approach to conduct a comprehensive assessment of wave energy for areas of interest and compared the performance of various WECs at the sites which were selected as superior for the construction of WEFs. Specifically, the method could be divided into three parts. In the first part, a comprehensive assessment of the North Indian Ocean wave characteristics was undertaken. Then, we identified the sites for WEFs in the nearshore areas considering water depth limitations, development potential and social conditions in the second part. In the third part, we analyzed the performance of various WECs at each site and selected the optimal device for each site.

### 3.1 Calculation method of richness index and stability index

In general, the analysis of wave energy characteristics and the quantification of wave energy resources are needed in a wave energy assessment. Specifically, it is necessary to analyze the richness and stability of wave energy. The most common parameter to quantify wave energy resources is the wave power density, as it reflects the richness of wave energy resources directly. We can get access to obtaining the spatial distribution of wave energy and determining the areas with relatively abundant wave energy by comparing the magnitudes of wave power density in the target areas. In order to obtain more accurate results, we employed the method suitable for all water depths to calculate the wave power density proposed by Wan et al. (2020) in this paper. Wave power density ( $P_w$ ) is calculated by using the following

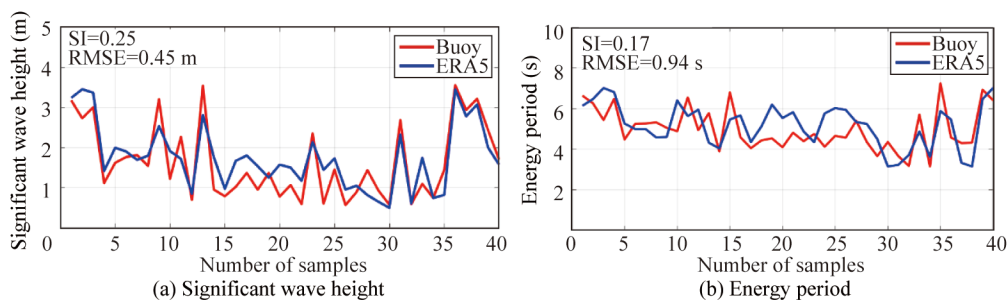


Fig. 2. Comparisons of ERA5 data and buoy data.

formula:

$$P_w = \bar{E} \left[ \frac{gT_e}{2\pi} \tanh(kd) \right] P_* \tag{1}$$

where,  $\bar{E}$  is the wave energy density,  $g$  is the gravitational acceleration,  $k$  is the wave number,  $d$  is the water depth, and  $P_*$  is an intermediate parameter. Refer to Wan et al. (2020) for the specific calculation process and other details.

When analyzing the feasibility of wave energy development, the time-varying characteristic is another important factor that must be considered. While abundant wave energy resources are suitable for exploitation and utilization, stable wave energy resources reduce the difficulty in actual development projects. Unstable wave energy resources not only reduce conversion efficiency, but also pose a significant threat to the safety of devices. The coefficient of variation of wave power density is generally used to represent the temporal wave power fluctuation. In general, the smaller the coefficient of variation is, the more stable the wave energy will be. The coefficient of variation can be obtained from the following equation:

$$C_V = \frac{\sqrt{\frac{1}{N} \sum_{i=1}^N (P_w - \bar{P}_w)^2}}{\bar{P}_w} \tag{2}$$

where  $C_V$  is the coefficient of variation,  $P_w$  is the wave power density,  $\bar{P}_w$  is the average of the wave power density, and  $N$  is the number of samples.

### 3.2 Method of site identification

As wave energy resources are not uniformly distributed in the North Indian Ocean, we need to select the small areas with abundant wave energy from the initial sea area and determine the sites considered as superior for constructing WEFs. In order to make the selection of WEF sites as reasonable as possible and obtain continuous energy output, we need to comprehensively consider wave energy characteristics, geographical features and socio-economic conditions and other aspects. For this purpose, we need to carry out site selection in two steps. In the first step, we used the regional division method proposed by Wan et al. (2020) to grade the coastal small areas of interest. Specifically, the quantitative division coefficient is used to indicate the development level of energy in the study area, and it is expressed as:

$$C_{QD} = P_w T_{E,w} C_{I,w} \tag{3}$$

where  $C_{QD}$  is the quantitative division coefficient,  $P_w$  repre-

sents the annual average of wave power density,  $T_{E,w}$  represents annual effective wave time and  $C_{I,w}$  represents potential installed capacity. In general, the larger the value of  $C_{QD}$  in a certain small area, the higher the potential development level of wave energy. In order to facilitate the selection of ideal development areas, five levels have been set based on the values of  $C_{QD}$ , which represent the levels of wave energy development potential in turn. The thresholds are calculated according to the method used by Wan et al. (2020). The specific thresholds are shown in Table 1. Thresholds such as  $m_1, n_1, p_1$  and  $q_1$  in the table are calculated according to the indicators in the first row of the corresponding column. By taking  $m_1$  and  $m_2$  as examples, the intermediate variable is obtained by dividing the difference between the maximum  $P_w$  and the minimum  $P_w$  by five,  $m_1$  is the minimum  $P_w$  plus twice the intermediate variable,  $m_2$  is  $P_w$  plus twice the intermediate variable, and so on.

After screening out the ideal development areas from the initial study area, the locations of WEF sites need to be determined, taking into consideration various aspects, such as  $C_{QD}$  values, socio-economic conditions, water depth and distance offshore. The reference weighting of the relevant factors should be adjusted for different areas to make the sites identification more scientific and reasonable.

### 3.3 WEC performance evaluation method

After completing the site identification, we should analyze the performance of various WECs at each site and select the optimal device for each WEF site. In the paper, we studied the performance and conversion efficiency of eight WECs.

Matching the most suitable WEC for a certain site depends on numerous aspects, so we should select appropriate performance indices to compare the WECs. According to the calculation results of each index, the adaptability of each WEC is evaluated, and the most suitable device is matched for the target site. As the ultimate objective of construction of WEFs is to generate electricity, the basic parameter for evaluating the performance of a WEC would be the mean power output, which is calculated as follows:

$$P_e = \sum_{i=1}^{nT} \sum_{j=1}^{nH} P_{ij} \times f_{ij} \tag{4}$$

where  $P_e$  is the mean power output (kW),  $P_{ij}$  is the power output of the WEC under different wave conditions, and  $f_{ij}$  is the occurrence frequency of each wave condition.

The capacity factor is another vital indicator that cannot

**Table 1** Criterion of the regional division

Grade	$P_w$ (kW/m)	$T_{E,w}$ (h)	$C_{I,w}$ ( $\times 10^7$ kW)	$C_{QD}$	Suitability level
1	$< m_1$	$< n_1$	$< p_1$	$< q_1$	Poor
2	$m_1 - m_2$	$n_1 - n_2$	$p_1 - p_2$	$q_1 - q_2$	Available
3	$m_2 - m_3$	$n_2 - n_3$	$p_2 - p_3$	$q_2 - q_3$	Good
4	$m_3 - m_4$	$n_3 - n_4$	$p_3 - p_4$	$q_3 - q_4$	Better
5	$> m_4$	$> n_4$	$> p_4$	$> q_4$	Best

be ignored. It indicates the average usage of the installed capacity of a WEC by the ratio between the average power output and the rated. Concretely, it can be defined as:

$$f_C = \frac{P_e}{P_R} \times 100, \quad (5)$$

where  $f_C$  is the capacity factor (%) and  $P_R$  is the rated power.

The capture width ratio represents the ability of a WEC to capture wave energy. Compared with the capture width, it also reduces the impact of the size of a device on energy output, and it is of great help to our follow-up research. The specific calculation methods are as follows:

$$R_{CW} = \frac{W_C}{D_m} \times 100, \quad (6)$$

where  $R_{CW}$  is the capture width ratio (%),  $W_C$  is the capture width and its calculation refers to the method used by Wan et al. (2020), and  $D_m$  is the characteristic size of each WEC. The main dimensions of the WECs are shown in Table 2.

**Table 2** Basic parameters of the WECs

Device	Rated power $P_R$ (kW)	Suited water depth (m)	$D_m$ (m)
AquaBuoy	250	>50	20
Archimedes Wave Swing	2000	40–100	144
Pelamis	750	50–70	180
Wave Star	600	Nearshore	70
Wave Dragon	7000	30–50	300
CETO	260	20–50	7
Oceantec	500	50–100	52
Reference Model 5	360	50–100	45

By comparing the results of the above three indicators, the most suitable WEC for each site can be determined. In general, the greater the value of the indicator, the higher the energy gain of the WEC at the site. The second part in this section is the site assessment. To put this in another way, we are supposed to analyze the wave energy characteristics at each site in the hope of providing guidance for the installation and deployment of WECs in the future. At the same site, the amount of energy that can be harvested by the WECs varies over time, considering that the WECs have different conversion efficiencies under different wave conditions. Therefore, in order to obtain the maximum power output, it is necessary to study the distribution of wave energy at each site according to the wave conditions.

The wave energy characteristics of a certain sea area can be described by the obtained parameters of significant wave height, wave energy period and wave power density. By comparing the values, we can have a preliminary understanding of the wave energy characteristics of a certain site. Stable wave conditions are conducive to improve energy output efficiency of WECs and disorder wave conditions will seriously affect the conversion efficiency of WECs. Furthermore, it is difficult to visually represent the wave

energy status of a site by only comparing the parameter values, and it is impossible to select stable wave conditions. In face of this circumstance, combined scatter and energy diagrams are used to describe the contribution of different wave conditions to wave energy, which not only makes the wave energy characteristics of WEF sites visualized, but also reveals the real sea states of each site, providing intuitive scientific guidance for the setting of WECs.

## 4 Results and discussion

### 4.1 Temporal and spatial distributions of wave power density

Wave power density is one of the most important indicators to evaluate the richness of wave energy resource in a certain region and show the spatial distribution of wave energy. Zheng and Li (2018) have proposed that when wave power density  $P_w$  is larger than 2 kW/m, the wave resources are available. The region with  $P_w$  larger than 20 kW/m is believed to be the rich area of wave energy resources. Therefore, we calculated the annual and seasonal averages of wave power density in the whole North Indian Ocean from 1999 to 2018 and the corresponding spatial distributions are shown in Fig. 3. Because of geographical location and topography, the climate in the North Indian Ocean region is severely affected by sea-route interactions, resulting in a significant monsoon climate. The northeast monsoon prevails from November to March of the following year, and the southwest monsoon prevails from May to September. Furthermore, the southwest monsoon is stronger and wider than the northeast monsoon. April and October are the months of monsoon transition, thus the wave energy resources in the North Indian Ocean have obvious regional differences and seasonal differences.

As shown in Fig. 3a, it can be seen that the averages of wave power density  $P_w$  in most areas of the North Indian Ocean exceed 10 kW/m, so the wave energy resources in the North Indian Ocean are available. However, regional differences are seen: the areas with extremely rich wave energy resources are identified in the Arabian Sea, the Bay of Bengal and the Somali Basin. Furthermore, the values in the Somali Basin are slightly lower than that in the other two areas. According to the values in Figs. 3b–3e, we can also find that there are significant seasonal differences in the North Indian Ocean. The wave energy resources are the richest in summer, with  $P_w$  above 10 kW/m in almost the entire large area. The second is autumn, followed by spring and winter, which is due to the summer southwest monsoon. In summer,  $P_w$  in the entire region of the Arabian Sea is larger than 20 kW/m and the values of some regions even exceed 50 kW/m. Meanwhile,  $P_w$  in most areas of the Bay of Bengal and the Somali Basin surpasses 20 kW/m. In contrast, wave energy resources in winter are a little insufficient owing to the northeast monsoon, which are weaker than that of the southwest monsoon. Nevertheless, wave energy

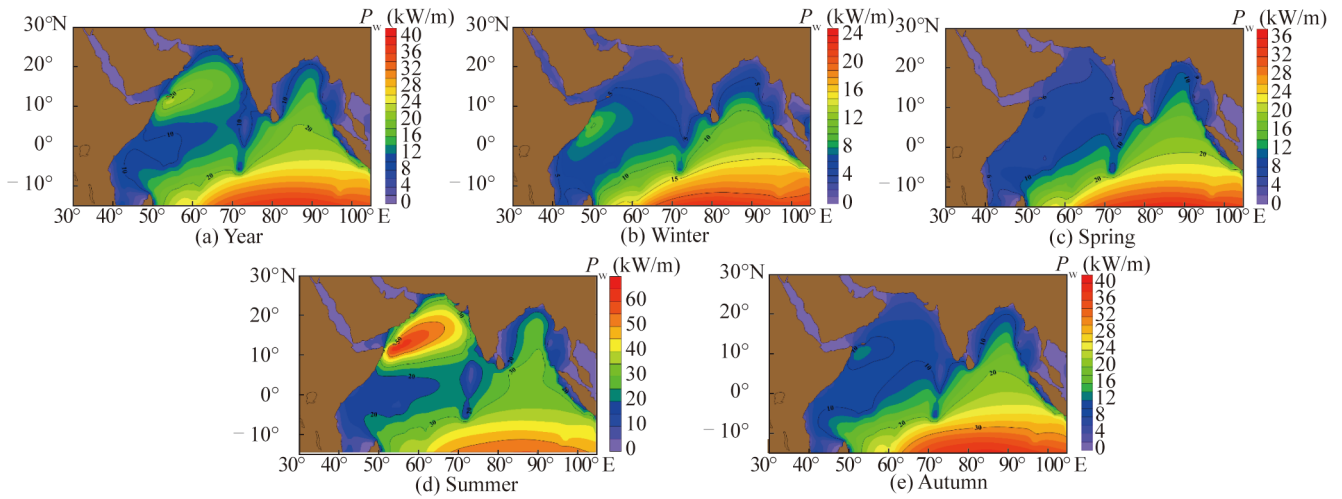


**Fig. 3.** Spatial distribution maps of wave power density.

resources in winter are also available with  $P_w$  above 2 kW/m throughout the North Indian Ocean. Spring and autumn are monsoon transition seasons. Although the wind is not as strong as that in summer, the wave power density in these two seasons is slightly higher than that in winter. The spatial distribution of  $P_w$  in spring is similar to that in autumn, and the area with large  $P_w$  is primarily found in the Bay of Bengal. In monsoon transition seasons, the influence of southwest monsoon on wave energy is slightly larger, so the values in autumn are a bit higher than those in spring.

In general, the North Indian Ocean has abundant wave energy resources with the average annual  $P_w$  of the Bay of Bengal, the Arabian Sea and the Somali Basin being above 10 kW/m, and it is an ideal development area of wave energy resources. In addition, pronounce seasonal variations in the North Indian Ocean are present and the wave energy resources in summer are the richest, which makes summer the key period for a wave energy development.

#### 4.2 Stability of wave energy resources

Cornett (2008) proposed that stable wave energy is advantageous for exploitation and utilization. When considering wave energy exploitation and wave power plants construction, stability is an important factor that cannot be ignored. In this paper, we calculated the annual and seasonal coefficients of variation ( $C_V$ ) by using the wave power density with the time interval of 6 h from 1999 to 2018. And the stability of wave energy in the North Indian Ocean is presented by using the values of  $C_V$  (Figs. 4a–4e). The smaller the values of  $C_V$ , the more stable the wave energy is in the target area. As shown in Fig. 4, wave power density has evident regional and temporal differences. From the distribution map of the annual  $C_V$ , we can find that the stability of wave energy resources in the Somali Basin is the best where the values of  $C_V$  are below 0.7 on the whole, followed by the Bay of Bengal with the values of  $C_V$  being generally smaller than 1. And then, the stability is relatively poor in the Arabian

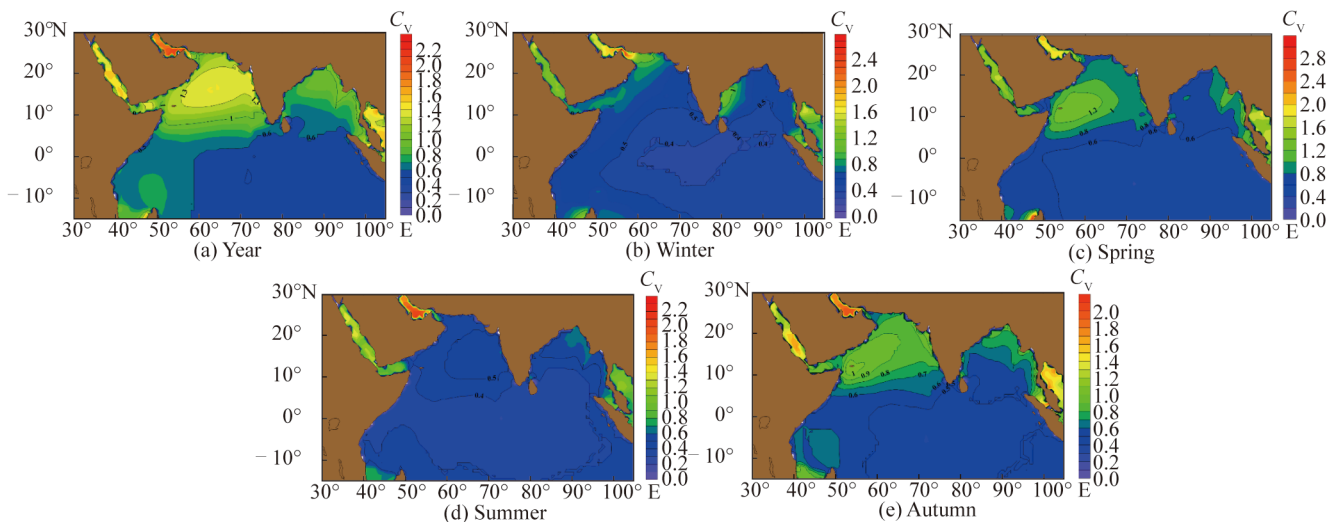


**Fig. 4.** Distribution maps of the coefficient of variation.



Sea, with the values of  $C_V$  generally larger than 1. Overall, the wave energy in the North Indian Ocean has good stability, which is suitable for the development of WEFs. But there are also certain regional and temporal differences. In spring, except for the Arabian Sea, the values of  $C_V$  in the other areas of the North Indian Ocean are below 0.8. In summer, wave energy is most stable, with the values of  $C_V$  being smaller than 0.6 integrally. Furthermore, wave energy is the most abundant in summer, thus summer should be regarded as the key season for wave energy development. The spatial distribution of  $C_V$  in autumn is similar to the annual  $C_V$ , and it is below 0.9 as a whole. Compared with spring and summer, the stability of wave energy in autumn is slightly worse. In winter, the stability of wave energy in the North Indian Ocean is good, and the values of  $C_V$  in the most regions are smaller than 0.7. However, the wave energy resources are not particularly enriched in this period, so winter is not an ideal season for developing wave energy.

#### 4.3 Selection of the WEF sites in the nearshore areas of the North Indian Ocean

Generally, with the increase of offshore distance, the wave energy resources will be more abundant, that is, the wave energy resources in the deep-water areas far from the shore will be richer than those in the nearshore areas. But it must be pointed out that the installation of WECs in offshore deep-water areas is particularly complex, and the cost of installation and subsequent maintenance will be very expensive. At present, most of the WECs are only suitable for nearshore shallow water areas. Therefore, in this study, we mainly concentrate on the wave energy potential in the nearshore areas. The North Indian Ocean is so vast that regional differences cannot be ignored. For this purpose, we divided the whole nearshore area into three parts (the Bay of Bengal, the Arabian Sea and the Somali Basin) for analysis. First, we continuously selected 57, 72, and 32 small areas in the coastal waters of the Bay of Bengal, Arabian Sea, and Somali Basin, respectively. In addition, the spatial resolution of these small areas is  $1^\circ \times 1^\circ$ , as shown in Figs. 5–7.

For the selected small coastal areas of interest, we carried

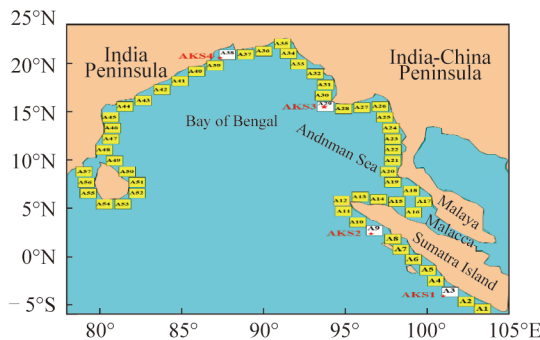


Fig. 5. The Bay of Bengal.

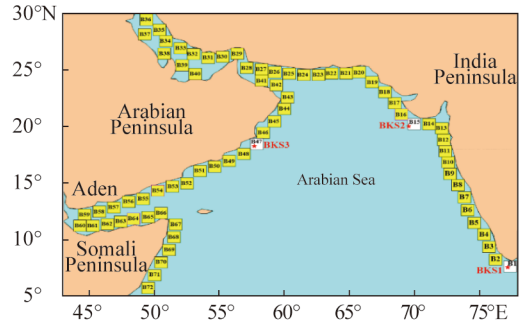


Fig. 6. The Arabian Sea.

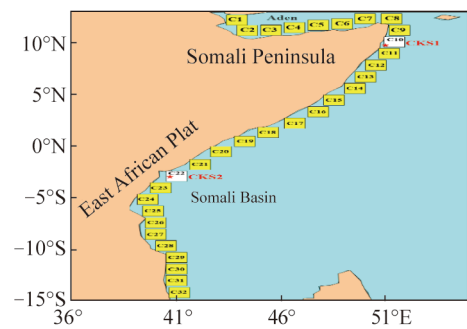


Fig. 7. The Somali Basin.

out regional grade division using the regional division method by Wan et al. (2020). The quantitative division coefficient ( $C_{QD}$ ) was used as the index to indicate the development level of energy in the study area, and the ranges of the threshold values differed among various small areas. The regional grade standards of the Bay of Bengal, the Arabian Sea and the Somali Basin are shown in Table 3. The corresponding threshold ranges of  $C_{QD}$  are different for the small areas selected from different sea areas, even if their grades of development potential are the same.

Generally, small areas with development potential level above 3 can be considered promising. The higher the development potential level is, the richer the wave energy resources in the region are. However, the development potential level is just one of the numerous factors to be considered in the site selection of a WEF. In view of the practical wave energy development project, we should also consider the development cost and social conditions. The potential wave energy in some regions is not most abundant, but there is huge energy demand because of its proximity to residential districts. If submarine cables are used to transmit electricity from areas with the highest development potential of wave energy, the transmission costs will be extremely high. Therefore, we should comprehensively consider the development potential, operation costs and geographical location to make reasonable decisions to select the ideal development areas of wave energy. In addition, WECs have the limitation of water depth at which they can operate, and most of the WECs only work in shallow coastal waters at present.

**Table 3** Regional grade standards of three sea areas

Grade	$P_w$ (kW/m)	$T_{E,w}$ (h)	$C_{L,w}$ ( $\times 10^7$ kW)	$C_{QD}$ ( $\times 10^{11}$ )	Suitability level
The Bay of Bengal					
1	< 4.74	< 1756	< 0.664	< 0.553	Poor
2	4.74–9.18	1756–3489	0.664–1.118	0.553–3.581	Available
3	9.18–13.62	3489–5222	1.118–1.572	3.581–11.181	Good
4	13.62–18.06	5222–6955	1.572–2.026	11.181–25.448	Better
5	> 18.06	> 6955	> 2.026	> 25.448	Best
The Arabian Sea					
1	< 3.82	< 1713	< 1.00	< 0.654	Poor
2	3.82–7.17	1713–3315	1.00–1.80	0.654–4.278	Available
3	7.17–10.52	3315–4917	1.80–2.60	4.278–13.449	Good
4	10.52–13.87	4917–6519	2.60–3.40	13.449–30.742	Better
5	> 13.87	> 6519	> 3.40	> 30.742	Best
The Somali Basin					
1	< 4.28	< 2286	< 1.428	< 1.397	Poor
2	4.28–7.48	2286–3710	1.428–2.106	1.397–5.844	Available
3	7.48–10.68	3710–5234	2.106–2.784	5.844–15.562	Good
4	10.68–13.88	5134–6558	2.784–3.462	15.562–31.513	Better
5	> 13.88	> 6558	> 3.462	> 31.513	Best

Therefore, when selecting the ideal development areas and the WEF sites, water depth is also a factor that cannot be ignored. In consideration of various factors, the results are represented in Figs. 5–7.

After comprehensive consideration, we have selected four small areas with the most potential for development in the Bay of Bengal, namely A3, A9, A29 and A38. Among them, the development level of A3 area is 5, and the corresponding  $C_{QD}$  is 32.912. The development level of A9 area is 3, and the corresponding  $C_{QD}$  is 6.481. The development level of A29 area is 3, and the corresponding  $C_{QD}$  is 4.043. The development level of A38 area is 3, and the corresponding  $C_{QD}$  is 5.78. Then, we have selected three small areas with the most potential for development in the Arabian Sea, namely B1, B15 and A47. Among them, the development level of B1 area is 4, and the corresponding  $C_{QD}$  value is 20.666. The development level of B15 area is 4, and the corresponding  $C_{QD}$  is 16.527. The development level of B47 area is 4, and the corresponding  $C_{QD}$  is 14.183. Afterwards, we have selected two small areas with the most potential for development in the Somali Basin, namely C10 and C22. Among them, the development level of C10 area is 5, and the corresponding  $C_{QD}$  is 50.381. The development level of C22 area is 3, and the corresponding  $C_{QD}$  is 11.608.

In the first stage of site selection, we selected the small areas with the most potential for development, which narrowed the scope of the initial study area and facilitated the subsequent work. In the second stage, what we need to do is to determine the sites of WEFs, for which we calculated the  $C_{QD}$  values of all grids within the small areas selected for wave energy development and checked the water depth at each grid. Then, among the grids that met the requirements of the operation depth of common WECs, the grid with the largest  $C_{QD}$  was selected as the location of the WEF sites.

When carrying out specific work, multiple aspects should be comprehensively considered, such as resource characteristics, environmental conditions and cost-effectiveness. Moreover, the reference weight of relevant factors can be appropriately adjusted for the regional differences in different seas, so that the selected WEF sites are more objective and reasonable, which has guiding significance for practical construction.

As the WECs could operate properly at each site, nine WEF sites were selected in the nearshore areas of the North Indian Ocean: AKS1, AKS2, AKS3, AKS4, BKS1, BKS2, BKS3, CKS1 and CKS2. The locations of the sites in ideal development areas are indicated by red pentagons in Figs. 5–7, respectively. The details of the WEF sites are exhibited in Table 4.

#### 4.4 Performance of WECs at WEF sites

When judging the feasibility of a wave energy project, it is crucial to evaluate the performance of common WECs at the WEF sites. To this end, we evaluated the performances of the WECs using three indicators mentioned in Section 3.1 and matched the most appropriate WEC for each promising WEF site. The three indicators are the mean power output, the capacity factor and the capture width ratio. The results of these indices for the WECs we studied at the sites are depicted in Tables 5–7.

At site AKS1, the highest value of mean power output was obtained from the AWS (288.32 kW), followed by the Wave Star (210.78 kW). Then the highest value of capacity factor was obtained from the Wave Star (0.35%), so was the capture width ratio (14.65%). Under comprehensive consideration, Wave Star was the most suitable WEC for site AKS1. Similar to site AKS1, Wave Star was also the most suitable WEC at site AKS2, with mean power output of



**Table 4** WEF sites information

Site	Longitude (°E)	Latitude (°N)	Water depth (m)	Sea area
AKS1	101.000	−4.125	58	The Bay of Bengal
AKS2	96.625	2.375	82	The Bay of Bengal
AKS3	93.750	15.500	62	The Bay of Bengal
AKS4	87.375	20.625	29	The Bay of Bengal
BKS1	77.250	7.500	88	The Arabian Sea
BKS2	69.625	20.000	82	The Arabian Sea
BKS3	57.750	18.250	26	The Arabian Sea
CKS1	51.000	9.750	30	The Somali Basin
CKS2	40.750	−3.000	126	The Somali Basin

**Table 5** Mean power output of WECs for nine sites

Location	Mean power output $P_e$ (kW)							
	AquaBuoy	AWS	Pelamis	RM5	Wave Star	Wave Dragon	CETO	Oceantec
AKS1	29.99	288.32	74.25	70.37	210.78	–	–	77.76
AKS2	10.98	107.09	–	34.41	83.71	–	–	26.33
AKS3	8.96	36.44	38.22	33.75	93.29	–	–	74.49
AKS4	–	–	–	–	107.31	–	8.68	–
BKS1	20.29	92.26	–	56.85	174.93	–	–	118.11
BKS2	23.45	106.22	–	56.26	158.89	–	–	104.10
BKS3	–	–	–	–	158.50	–	14.04	–
CKS1	–	–	–	–	252.94	311.08	26.27	–
CKS2	10.52	–	–	–	145.27	–	–	–

**Table 6** Capacity factor of WECs for nine sites

Location	Capacity factor $f_c$ (%)							
	AquaBuoy	AWS	Pelamis	RM5	Wave Star	Wave Dragon	CETO	Oceantec
AKS1	0.12	0.11	0.10	0.20	0.35	–	–	0.16
AKS2	0.04	0.05	–	0.10	0.14	–	–	0.05
AKS3	0.04	0.02	0.05	0.09	0.16	–	–	0.15
AKS4	–	–	–	–	0.18	–	0.02	–
BKS1	0.08	0.05	–	0.16	0.29	–	–	0.24
BKS2	0.09	0.05	–	0.16	0.26	–	–	0.21
BKS3	–	–	–	–	0.26	–	0.03	–
CKS1	–	–	–	–	0.42	0.04	0.05	–
CKS2	0.04	–	–	–	0.24	–	–	–

**Table 7** Capture width ratio of WECs for nine sites

Location	Capture width ratio $R_{CW}$ (%)							
	AquaBuoy	AWS	Pelamis	RM5	Wave Star	Wave Dragon	CETO	Oceantec
AKS1	7.30	7.72	2.01	7.61	14.65	–	–	7.28
AKS2	5.72	7.75	–	7.97	12.46	–	–	5.28
AKS3	6.72	3.80	3.19	11.25	20.00	–	–	21.50
AKS4	–	–	–	–	17.13	–	1.87	–
BKS1	8.59	5.42	–	10.69	21.15	–	–	19.22
BKS2	8.97	5.64	–	9.56	17.36	–	–	15.31
BKS3	–	–	–	–	19.00	–	2.64	–
CKS1	–	–	–	–	20.42	0.75	2.86	–
CKS2	6.45	–	–	–	25.44	–	–	–

83.71 kW, capacity factor of 0.14% and capture width ratio of 12.46%. At site AKS3, of all the WECs that met the requirements, the three indexes of Wave Star were much higher than those of other devices, making Wave Star the best match for site AKS3. At site AKS4 and site BKS3, in

virtue of the limitation of water depth, only Wave Star and CETO met the operating conditions among the devices studied. In addition, the values of the Wave Star were obviously superior to those of the CETO. Hence, the Wave Star was also the most suitable WEC at site AKS4 and site BKS3,

with values of mean power output being 107.31 kW and 158.5 kW, values of capacity factor 0.18% and 0.26%, values of capture width ratio 17.13% and 19% respectively. Wave Star was also the most suitable WEC at site BKS1 and site BKS2. However, it was worth pointing out that the Oceantec ranked second and the values of Oceantec were slightly lower than those of Wave Star. As a result, Oceantec should also be regarded as an alternative. For site CKS1, we need to discuss it in two cases. When mainly considering the mean power output, Wave Dragon was the most suitable WEC with 311.08 kW. When dominated by capacity factor and capture width ratio, Wave Star was the best matching device with 0.42% and 20.42%. At site CKS2, all three indicators of the Wave Star were the highest, making Wave Star the best match for site CKS2. Overall, Wave Star was the most suitable WEC at most WEFs sites for the North Indian Ocean inshore waters.

#### 4.5 Wave energy distributions according to wave conditions

It is noteworthy that a WEC will have specific power within a certain wave condition range, and the power values in all wave conditions will form a power matrix. In addition, Bingölbali et al. (2020) have proposed that different wave conditions determined by combining significant wave heights in different ranges with different energy periods represent different wave climates. In order to determine the wave characteristics of each WEF site and provide reference for the subsequent deployment of WECs, scatter diagrams of  $H_s - T_e$  joint distributions were generated by using the ERA5 data from 1999 to 2018. As depicted in Fig. 8, the interval of significant wave height  $H_s$  we selected was 0.5 m, and the interval of energy period  $T_e$  was 1 s. Then we calculated the occurrences of different wave conditions and analyzed their contributions to the total annual wave energy density at each site. For the calculation process, please refer to Wan et al. (2020). In addition, the numbers in each bin

indicate the occurrence of corresponding wave conditions and the color bar denotes the percentage of energy in total energy under different wave conditions.

As seen from Fig. 8, the occurrence of wave conditions with  $H_s=1.5-2.0$  m and  $T_e=10-11$  s was the highest with 257 occurrences, which also contributed the highest to the total annual energy at site AKS1. In addition, the wave conditions which contributed greatly to the total energy corresponded to  $H_s=1.5-3.0$  m and  $T_e=8-13$  s, accounting for 83.09%. At site AKS2, the range of wave conditions with the highest occurrences was  $H_s=1.0-1.5$  m and  $T_e=10-11$  s, which differed from that with the largest contributions to the total energy density. The range of wave conditions with the highest contributions to total energy was  $H_s=1.0-2.0$  m and  $T_e=8-14$  s, accounting for 82.80%. The range of wave conditions that occurred most frequently at site AKS3 was  $H_s=0.5-1.0$  m and  $T_e=7-8$  s, with 181 occurrences. The range of wave conditions that contributed the most to the total energy density concentrated on  $H_s=1.5-2.0$  m and  $T_e=7-8$  s. In addition, the range of wave conditions which contributed greatly to the total energy corresponded to  $H_s=0.5-3.0$  m and  $T_e=7-10$  s, accounting for 77.58%. The range of wave conditions that occurred most frequently at site AKS4 was  $H_s=0.5-1.0$  m and  $T_e=9-10$  s with 129 occurrences. The greatest contributions of wave conditions were observed in the range of  $H_s=1.5-2.0$  m and  $T_e=8-9$  s. Furthermore, the range of wave conditions with large contributions to total energy density was  $H_s=0.5-2.5$  m and  $T_e=6-12$  s, accounting for 77.58%. Therefore, it is highly appropriate to develop WEFs in the Bay of Bengal, with the conditions contributing significantly to total wave energy density being mainly in the range of  $H_s=0.5-3.0$  m and  $T_e=8-14$  s. Furthermore, the wave conditions were also under storm protection, which is ideal for the construction and installation of WECs.

At the site BKS1 of the Arabian Sea, the occurrence of

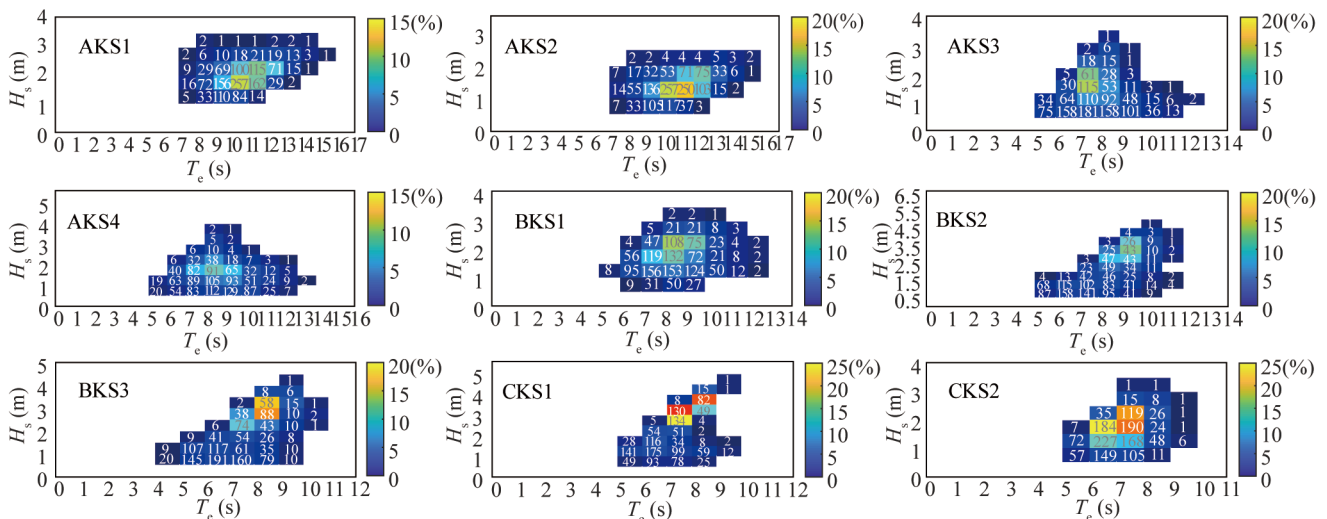


Fig. 8. Scatter diagrams of wave energy based on significant wave height and energy period for each site.

wave conditions with  $H_s=1.0\text{--}1.5$  m and  $T_e=7\text{--}8$  s was the highest with 156. The wave conditions which contributed the greatest to the total wave energy corresponded to  $H_s=2.0\text{--}2.5$  m and  $T_e=8\text{--}9$  s, with 108 occurrences. In addition, the wave conditions with large contributions to the total wave energy corresponded to  $H_s=1.0\text{--}3.0$  m and  $T_e=7\text{--}11$  s, accounting for 86.26% of the total energy density at the site BKS1. The highest occurrence of wave conditions was in the range of  $H_s=0.5\text{--}1.0$  m and  $T_e=6\text{--}7$  s at site BKS2, with 158 occurrences. Furthermore, the range of wave conditions that contributed the most to the total energy density concentrated on  $H_s=3.0\text{--}3.5$  m and  $T_e=9\text{--}10$  s. Further, the range of wave conditions with large contributions to total energy density was  $H_s=0.5\text{--}4.0$  m and  $T_e=8\text{--}11$  s, accounting for 75.44%. Coincidentally, the wave conditions with the highest occurrences of BKS3 was also in the range of  $H_s=0.5\text{--}1.0$  m and  $T_e=6\text{--}7$  s, with 191 occurrences. Furthermore, the range of wave conditions that contributed the most to the total energy density was  $H_s=2.5\text{--}3.0$  m and  $T_e=8\text{--}9$  s. In addition, the wave conditions which yielded large contributions corresponded to  $H_s=0.5\text{--}3.5$  m and  $T_e=7\text{--}10$  s, accounting for 79.40%. In short, the sea state with the highest occurrences at sites in the Arabian Sea was significantly lower than that with the largest energy contribution, which is suitable for the construction of WEFs.

In the Somali Basin, the wave conditions of  $H_s=1.0\text{--}1.5$  m and  $T_e=6\text{--}7$  s occurred 175 occurrences annually at site CKS1. The wave conditions of  $H_s=3.0\text{--}3.5$  m and  $T_e=7\text{--}8$  s contributed most to the total wave energy. In addition, the wave conditions which yielded large contributions to the total energy corresponded to  $H_s=0.5\text{--}4.0$  m and  $T_e=7\text{--}9$  s, accounting for 77.47% of the total energy. The range of wave conditions that contributed most to the total wave energy density at site CKS2 corresponded to  $H_s=1.5\text{--}2.0$  m and  $T_e=7\text{--}8$  s, which also happened to be the most frequent, with 190 occurrences. Further, the range of wave conditions with large contributions was  $H_s=0.5\text{--}2.5$  m and  $T_e=6\text{--}8$  s, accounting for 88.96% of the total wave energy. In comparison, the sea state of site CKS2 was mildly lower than that of site CKS1. At site CKS2, the wave conditions with the highest occurrences and the wave conditions with the largest contribution to the total energy were in the same range, which is more advantageous for the centralized capture and sustained supply of wave energy.

Overall, most of the wave conditions with high-frequency and large energy contributions at the proposed North Indian Ocean WEF sites were under storm protection. In addition, the proportion of wave conditions that contributed significantly to the total wave energy was very high, all over 75%. Moreover, at some sites, the wave condition ranges with the highest number of occurrences happened to be the ranges with the highest proportion of wave energy. It can be seen that the wave conditions in the nearshore areas of the North Indian Ocean are quite good, and the commercial develop-

ment of wave energy in the North Indian Ocean is highly promising.

#### 4.6 Directional distribution of wave energy

For the site selection of WEFs, the areas with relatively concentrated wave energy are generally selected. This is because the installation positions of WECs are relatively fixed, and more concentrated wave energy is more conducive to collection and conversion. Thus, the research on directionality of wave energy propagation plays a crucial role. Further, in practical engineering applications, the operation and maintenance of WECs is an issue that must be considered. Under high sea states, in order to protect the WECs, the equipment must be switched off, so the wave energy cannot continue to be captured and utilized. In this case, in order to study the concentration of wave energy propagation, we calculated and analyzed the proportions of wave energy in all directions at each site and plotted the annual wave power roses based on ERA5 wave data from 1999 to 2018. In this study, we also used the criterion proposed by Wan et al. (2020). When the significant wave height exceeds 3.0 m, the wave energy converters will enter storm protection mode and the wave energy during this period is not available. The wave rose diagrams for the full sea state and storm protection state at each site are shown in Fig. 9.

In the Bay of Bengal, energy was generated from the waves coming from S–SW (clockwise) at site AKS1. The percentage of energy in the main wave directions under the full sea state was about 94.49%. The energy in the main wave directions under the storm protection state was more concentrated, accounting for approximately 94.73%. At site AKS2, energy could mainly be generated from the waves coming from SSW–WSW. The percentage of energy in the main wave directions under the full sea state was about 99.03%, with 99.04% under storm protection state. Obviously, in addition to the concentrated wave energy at site AKS2, most of the wave energy was under storm protection state. The directions of the main wave power at site AKS3 were consistent with those of the site AKS2, but the proportion was slightly lower. The percentage of energy in the main wave directions under the full sea state was about 87.41%, with 86.85% under storm protection state. Compared with the above three sites, the dominant waves of site AKS4 were coming from S and SSW, which were more concentrated. The percentage of dominant wave power under the full sea state was 89.51%, with 90.40% under storm protection state.

In the Arabian Sea, except for the SW and WSW directions, the wave energy site BKS1 was also concentrated in S, SSW and W directions. Thus, wave energy at site BKS1 was not particularly concentrated. The percentage of energy in the main wave directions under the full sea state was about 83.35%. The percentage of energy in the main wave directions under the full sea state was about 83.16%. At site

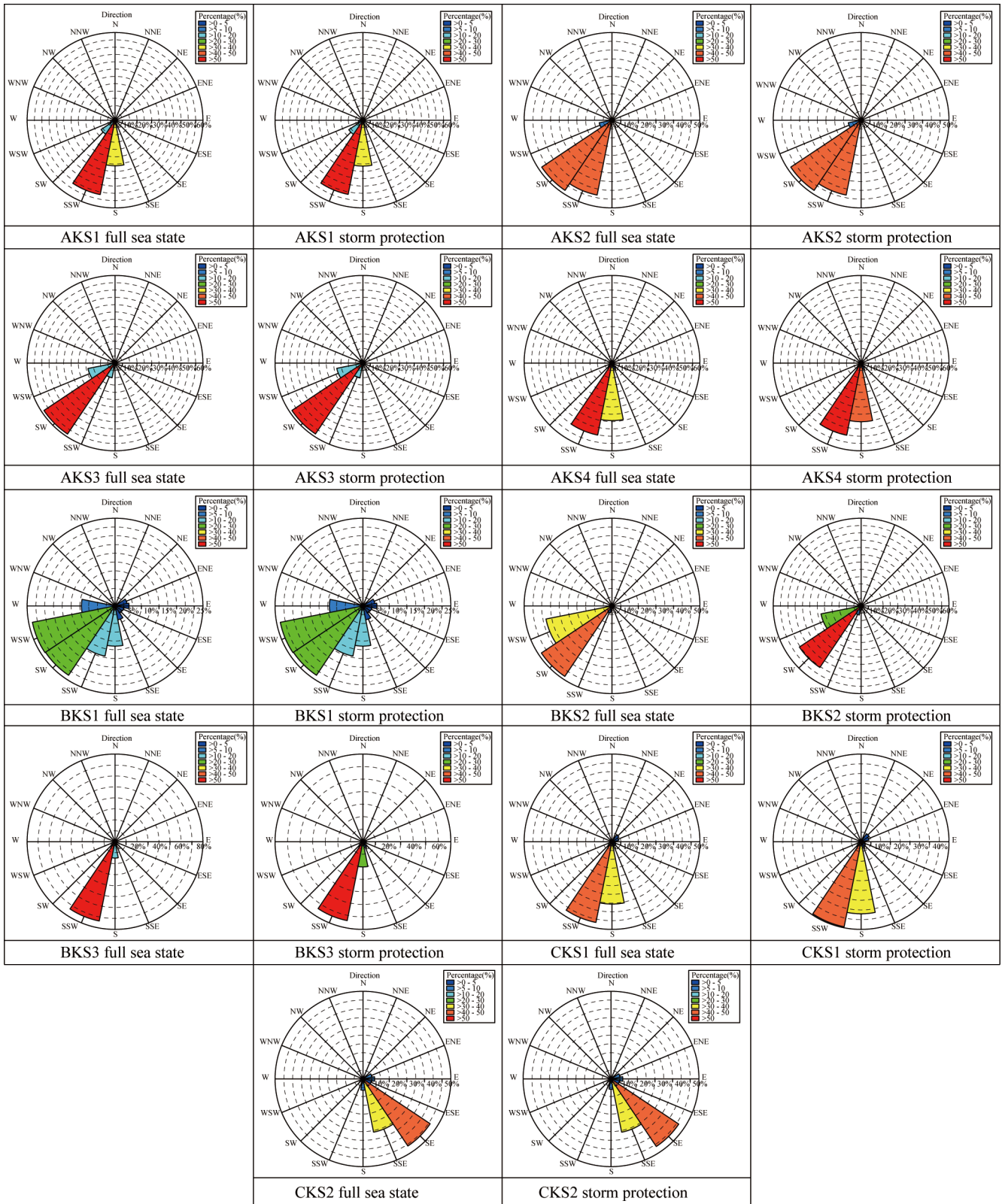


Fig. 9. Wave power rose diagrams for the full sea state and storm protection state at each key station.

BKS2, energy would be produced from waves coming from the SW–WSW direction. The percentage of energy coming from the SW–WSW direction under the full sea state was about 83.63%, with 78.58% under storm protection state. At

site BKS3, the wave energy mainly concentrated on direction SSW, and the proportion of wave energy under the full sea state was 88.62% with 84.33% under storm protection state.

In the Somali Basin, wave energy was concentrated in

two directions. Specifically, energy could be generated from waves in the direction S–SSW at site CKS1, while the dominant waves of site CKS2 were coming from the SE and SSE. At site CKS1, the percentage of energy in the main wave directions under the full sea state was about 82.69%. The proportion of wave energy in the main wave directions under the storm protection state was much lower, only 60.34%. At site CKS2, the percentage of energy in the main wave directions under the full sea state was about 76.90%. The energy in the main wave directions under the storm protection state was more concentrated, accounting for 77.26% approximately.

On the whole, the sea states in nearshore areas of the North Indian Ocean are quite low. The wave energy is extremely concentrated. At most sites, the dominant waves were coming from one or two directions, which provided reliable basis for the installation and deployment of the WECs in the future. Apart from BKS2 and CKS2 sites, all other sites in the North Indian nearshore waters had a large proportion of wave power in the SSW direction, therefore, SSW should be used as the key direction for the subsequent research.

## 5 Conclusions

In view of the important geographical location and superior resource conditions, we conducted an overall assessment of wave energy resources in the coastal area of the North Indian Ocean by using ERA5 data from 1999 to 2018. First, we analyzed the wave energy characteristics of the entire North Indian Ocean, including the richness and stability of wave energy resources. Then we selected the ideal development areas for wave energy and determined the sites considered as superior for the construction of WEFs. Finally, we analyzed the performance of eight WECs at all sites, matched the most appropriate WEC for each site, and assessed the wave energy characteristics of each site. The conclusions are as follows:

The wave energy resources in the North Indian Ocean are highly abundant and the annual average wave power density is almost above 10 kW/m, which is suitable for the development and utilization of wave energy resources. In addition, there are distinct seasonal variations due to the influence of monsoon climate. The wave energy resources in summer are more abundant than those in the other three seasons, so summer should be the key period of WEFs development.

In view of the rich wave energy resources in the coastal waters of the North Indian Ocean, we selected 9 small areas at a spatial resolution of  $1^\circ \times 1^\circ$  in the nearshore area of the North Indian Ocean as the ideal development areas of wave energy. Subsequently, the locations of WEF sites were determined according to the  $C_{QD}$  value, water depth and offshore distance, which provided guidance for the development of wave energy resources and the construction of WEFs in

the future.

Three indices including mean power output  $P_e$ , capacity factor  $f_C$ , and capture width ratio  $R_{CW}$  were used to evaluate the performance of the eight WECs at each site. It was found that the Wave Star matched most sites best in the nearshore areas of the North Indian Ocean. Then, the directionality of wave energy propagation of each site and the wave energy distributions based on significant wave height and energy period were studied. It is also found that the wave conditions range which contributed greatly to total wave energy were under storm protection and the dominant waves were coming from one or two directions. In addition, the proportion of wave conditions that contributed significantly to the total wave energy was very high, all over 75%. So, the energy accounts for a relatively high proportion and wave energy is very concentrated, which provided reference for the installation and deployment of WECs at each site in the future.

In general, the wave energy in the Northern Indian Ocean is very rich and stable, the directionality of wave energy propagation is relatively concentrated, and the sea states with high occurrence frequency and large contributions to the total wave energy are also relatively low, which is very suitable for the development of WEFs.

## References

- Ahn, S., Haas, K.A. and Neary, V.S., 2020. Wave energy resource characterization and assessment for coastal waters of the United States, *Applied Energy*, 267, 114922.
- Akpınar, A. and İhsan Kömürçü, M., 2013. Assessment of wave energy resource of the black sea based on 15-year numerical hindcast data, *Applied Energy*, 101, 502–512.
- Amarouche, K., Akpınar, A., El Islam Bachari, N. and Houma, F., 2020. Wave energy resource assessment along the Algerian coast based on 39-year wave hindcast, *Renewable Energy*, 153, 840–860.
- Ayob, M.N., Castellucci, V. and Waters, R., 2017. Wave energy potential and 1–50 TWh scenarios for the Nordic synchronous grid, *Renewable Energy*, 101, 462–466.
- Bertram, D.V., Tarighaleslami, A.H., Walmsley, M.R.W., Atkins, M.J. and Glasgow, G.D.E., 2020. A systematic approach for selecting suitable wave energy converters for potential wave energy farm sites, *Renewable and Sustainable Energy Reviews*, 132, 110011.
- Besio, G., Mentaschi, L. and Mazzino, A., 2016. Wave energy resource assessment in the Mediterranean Sea on the basis of a 35-year hindcast, *Energy*, 94, 50–63.
- Bingölbali, B., Jafali, H., Akpınar, A. and Bekiroğlu, S., 2020. Wave energy potential and variability for the South West coasts of the Black Sea: The WEB-based wave energy atlas, *Renewable Energy*, 154, 136–150.
- Chiu, F.C., Huang, W.Y. and Tiao, W.C., 2013. The spatial and temporal characteristics of the wave energy resources around Taiwan, *Renewable Energy*, 52, 218–221.
- Cornett, A.M., 2008. A global wave energy resource assessment, *Proceedings of the Eighteenth International Offshore and Polar Conference*, Vancouver, BC Canada.
- Dalton, G.J., Alcorn, R. and Lewis, T., 2010. Case study feasibility analysis of the Pelamis wave energy convertor in Ireland, Portugal and North America, *Renewable Energy*, 35(2), 443–455.

- De Andres, A., Guanche, R., Vidal, C. and Losada, I.J., 2015. Adaptability of a generic wave energy converter to different climate conditions, *Renewable Energy*, 78, 322–333.
- García-Medina, G., Özkan Haller, H.T. and Ruggiero, P., 2014. Wave resource assessment in Oregon and southwest Washington, USA, *Renewable Energy*, 64, 203–214.
- Hersbach, H., Bell, B., Berrisford, P., Hirahara, S., Horányi, A., Muñoz-Sabater, J., Nicolas, J., Peubey, C., Radu, R., Schepers, D., Simmons, A., Soci, C., Abdalla, S., Abellan, X., Balsamo, G., Bechtold, P., Biavati, G., Bidlot, J., Bonavita, M., De Chiara, G., Dahlgren, P., Dee, D., Diamantakis, M., Dragani, R., Flemming, J., Forbes, R., Fuentes, M., Geer, A., Haimberger, L., Healy, S., Hogan, R.J., Hólm, E., Janisková, M., Keeley, S., Laloyaux, P., Lopez, P., Lupu, C., Radnoti, G., de Rosnay, P., Rozum, I., Vamborg, F., Villaume, S. and Thépaut, J.N., 2020. The ERA5 global reanalysis, *Quarterly Journal of the Royal Meteorological Society*, 146(730), 1999–2049.
- Iglesias, G., Carballo, R., 2010. Offshore and inshore wave energy assessment: Asturias (N Spain), *Energy*, 35(5), 1964–1972.
- Iglesias, G., López, M., Carballo, R., Castro, A., Fraguera, J. and Frigaard, P., 2009. Wave energy potential in Galicia (NW Spain), *Renewable Energy*, 34(11), 2323–2333.
- Koca, K., Kortenhuis, A., Oumeraci, H., Zanuttigh, B., Angelelli, E., Cantù, M., Suffredini, R. and Franceschi, G., 2013. Recent advances in the development of wave energy converters, *Proceedings of the 10th European Wave and Tidal Energy Conference*, IEEE, Aalborg, Denmark.
- Langodan, S., Viswanadhapalli, Y., Dasari, H.P., Knio, O. and Hoteit, I., 2016. A high-resolution assessment of wind and wave energy potentials in the Red Sea, *Applied Energy*, 181, 244–255.
- Liberti, L., Carillo, A. and Sannino, G., 2013. Wave energy resource assessment in the Mediterranean, the Italian perspective, *Renewable Energy*, 50, 938–949.
- Lisboa, R.C., Teixeira, P.R.F. and Fortes, C.J., 2017. Numerical evaluation of wave energy potential in the South of Brazil, *Energy*, 121, 176–184.
- Mørk, G., Barstow, S., Kabuth, A. and Pontes, M.T., 2010. Assessing the global wave energy potential, *Proceedings of the ASME 2010 29th International Conference on Ocean, Offshore and Arctic Engineering*, ASME, Shanghai, China.
- Patel, R.P., Nagababu, G., Arun Kumar, S.V.V., Seemanth, S. and Kachhwaha, S.S., 2020. Wave resource assessment and wave energy exploitation along the Indian coast, *Ocean Engineering*, 217, 107834.
- Reguero, B.G., Losada, I.J. and Méndez, F.J., 2015. A global wave power resource and its seasonal, interannual and long-term variability, *Applied Energy*, 148, 366–380.
- Ribeiro, A.S., DeCastro, M., Costoya, X., Rusu, L., Dias, J.M. and Gomez-Gesteira, M., 2021. A Delphi method to classify wave energy resource for the 21st century: Application to the NW Iberian peninsula, *Energy*, 235, 121396.
- Rusu, E., 2014. Evaluation of the wave energy conversion efficiency in various coastal environments, *Energies*, 7(6), 4002–4018.
- Rusu, L., 2019. Evaluation of the near future wave energy resources in the Black Sea under two climate scenarios, *Renewable Energy*, 142, 137–146.
- Saket, A. and Etemad-Shahidi, A., 2012. Wave energy potential along the northern coasts of the gulf of Oman, Iran, *Renewable Energy*, 40(1), 90–97.
- Silva, D., Rusu, E. and Soares, C.G., 2013. Evaluation of various technologies for wave energy conversion in the Portuguese Nearshore, *Energies*, 6(3), 1344–1364.
- Vannucchi, V. and Cappiotti, L., 2016. Wave energy assessment and performance estimation of state of the art wave energy converters in Italian hotspots, *Sustainability*, 8(12), 1300.
- Wahyudie, A., Susilo, T.B., Alaryani, F., Nandar, C.S.A., Jama, M.A., Daher, A. and Shareef, H., 2020. Wave power assessment in the middle part of the southern coast of Java Island, *Energies*, 13(10), 2633.
- Wan, Y., Zheng, C.W., Li, L.G., Dai, Y.S., Esteban, M.D., López-Gutiérrez, J.S., Qu, X.J. and Zhang, X.Y., 2020. Wave energy assessment related to wave energy converters in the coastal waters of China, *Energy*, 202, 117741.
- Zheng, C.W., 2021. Global oceanic wave energy resource dataset—with the Maritime Silk Road as a case study, *Renewable Energy*, 169, 843–854.
- Zheng, C.W. and Li, C.Y., 2017. 21<sup>st</sup> century maritime silk road: big data construction of new marine resources: Wave energy as a case study, *Ocean Development and Management*, 34(12), 61–65. (in Chinese)
- Zheng, C.W. and Li, C.Y., 2018. Overview of site selection difficulties for marine new energy power plant and suggestions: Wave energy case study, *Journal of Harbin Engineering University*, 39(2), 200–206. (in Chinese)
- Zheng, C.W., Pan, J. and Li, J.X., 2013. Assessing the China Sea wind energy and wave energy resources from 1988 to 2009, *Ocean Engineering*, 65, 39–48.
- Zheng, C.W., Wu, G.X., Chen, X., Wang, Q., Gao, Z.S., Chen, Y.G. and Luo, X., 2019. CMIP5-based wave energy projection: Case studies of the South China Sea and the East China Sea, *IEEE Access*, 7, 82753–82763.